Electroresistance Effect in Ferroelectric Tunnel Junctions with Symmetric Electrodes

Daniel I. Bilc,[†,⊥] Frederico D. Novaes,[‡,§,⊥] Jorge Íñiguez,[‡] Pablo Ordejón,[§] and Philippe Ghosez[†,*]

[†]Physique Théorique des Matériaux, Université de Liège, 4000 Liège, Belgium, [‡]Institut de Ciència de Materials de Barcelona (ICMAB-CSIC), Campus UAB, 08193 Bellaterra, Spain, and [§]Centre d'Investigacions en Nanociència i Nanotecnologia—CIN2 (CSIC-ICN), Campus UAB, 08193 Bellaterra, Spain. [⊥]These authors contributed equally to this work.

ABSTRACT

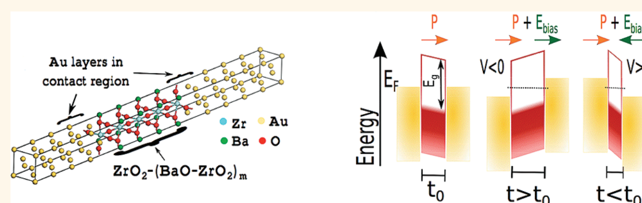

Understanding the effects that govern electronic transport in ferroelectric tunnel junctions (FTJs) is of vital importance to improve the efficiency of devices such as ferroelectric memories with nondestructive readout. However, our current knowledge (typically based on simple semiempirical models or first-principles calculations restricted to the limit of zero bias) remains partial, which may hinder the development of more efficient systems. For example, nowadays it is commonly believed that the tunnel electroresistance (TER) effect exploited in such devices mandatorily requires, to be sizable, the use of two different electrodes, with related potential drawbacks concerning retention time, switching, and polarization imprint. In contrast, here we demonstrate at the first-principles level that large TER values of about 200% can be achieved under finite bias in a prototypical FTJ with symmetric electrodes. Our atomistic approach allows us to quantify the contribution of different microscopic mechanisms to the electroresistance, revealing the dominant role of the inverse piezoelectric response of the ferroelectric. On the basis of our analysis, we provide a critical discussion of the semiempirical models traditionally used to describe FTJs.

KEYWORDS: ferroelectric tunnel junction · first-principles calculations

The concept of ferroelectric tunnel junction (FTJ) was already proposed by Esaki in 1971,[1] but its practical realization has for a long time been hampered by experimental limitations. At the time of Esaki's proposal, it was not even clear whether ferroelectricity would be preserved in the range of barrier thicknesses required for tunneling. Only recently has it been established that layers of only a few nanometers can remain ferroelectric, provided the electrical and mechanical boundary conditions are adequate.[2,3]

Together with the advances in the growth of high-quality oxide heterostructures, the interest in FTJs naturally re-emerged. A large asymmetry in the tunnel current under polarization reversal was first measured in a 6 nm thick $SrRuO_3/Pb(Zr_{0.52}Ti_{0.48})O_3/Pt$ FTJ (although the measured current might not be in the direct tunneling regime in this case)[4] and then also in a 2 nm thick $La_{2/3}Sr_{1/3}MnO_3/La_{0.1}Bi_{0.9}MnO_3/Au$ multiferroic junction.[5] The related tunnel electroresistance (TER) effect, that is, the dependence of the resistance on the orientation of the polarization of the ferroelectric, is not only of academic interest but also valuable for practical applications. The most obvious one pertains to ferroelectric random access memories (FE-RAMs)[6] based on ferroelectric capacitors in which measurement of the tunneling current would allow for nondestructive readout of the polarization state. Recently, using conductive atomic force microscopy, García *et al.*[7] reported a giant TER of 75.000% across a 3 nm thick $BaTiO_3$ barrier and demonstrated scalability down to lateral sizes compatible with storage densities greater than 16 Gbit in.$^{-2}$. Similar results were reported on other systems,[8−13] motivating further exploration of the interplay between tunneling and ferroelectricity.

Presently, it is commonly accepted that, in order to obtain a sizable TER, it is mandatory to have *asymmetric* FTJs (a-FTJs in the following), that is, junctions involving two different metallic electrodes.[14] Such a belief seems to rely on theoretical arguments assuming that the magnitude of the tunnel current is essentially controlled by the mean barrier height, a parameter that does not change upon polarization switching in *symmetric* junctions, that is, FTJs with identical left and right electrodes (s-FTJs in the following). While recent experimental

* Address correspondence to Philippe.Ghosez@ulg.ac.be.

Received for review November 8, 2011 and accepted January 9, 2012.

Published online January 09, 2012
10.1021/nn2043324

© 2012 American Chemical Society

results are promising, the presence of two different electrodes in a-FTJs results in a preferred polarization orientation of the ferroelectric barrier, with related drawbacks concerning retention time, switching, and polarization imprint.[15] Thus, it is timely to question whether having asymmetric electrodes is really mandatory or, rather, whether the symmetry breaking induced by the polarization itself and already present in symmetric junctions might be sufficient to modulate the tunneling current. Here we give an answer to this fundamental question. We prove at the theoretical level that, contrary to the common belief, s-FTJs can indeed exhibit a large TER. Our fully first-principles approach makes it possible to quantify, for the first time, the different mechanisms contributing to the effect and opens new perspectives for the modeling and design of ferroelectric tunnel junctions.

For a long time, the theory of FTJs relied on semi-empirical approaches[14,16−18] that, while very useful, present serious limitations. As highlighted by Tsymbal and Kohlstedt,[19] describing FTJs faithfully constitutes a challenging problem that, beyond the correct quantum modeling of electron tunneling, requires to take simultaneously into account various effects, such as the electrostatic screening at the interfaces and the atomic (including strain) relaxations within the barrier and at the interfaces under applied voltage. Progress has been made recently toward a first-principles characterization of FTJs,[20−24] but the simulations have so far been restricted to the limit of zero bias.[25] This unsatisfactory situation can be partly attributed to the large computational cost associated with the simulations of such complex systems and phenomena but also to intrinsic limitations of density functional theory (DFT) methods.[2] DFT calculations within the usual local density (LDA) and generalized gradient (GGA) approximations systematically underestimate the band gap of typical ferroelectrics by a factor of about 2. Such a problem often becomes pathological in the simulation of FTJs, as it is common for DFT to locate the Fermi level of the metal in the vicinity of the conduction band of the ferroelectric barrier rather than well inside its gap.[26] Such an error results in computed Schottky barriers that are artificially too small, which in turn yields an overestimate of the tunnel current and makes it impossible to simulate the FTJ under a significant bias without incurring in Zener breakdown.

In order to circumvent those problems, we searched for a model ferroelectric system that exhibits, in a DFT-LDA simulation, the same characteristics as a typical real FTJ. We selected $BaZrO_3$, a wide band gap perovskite oxide that, although not ferroelectric in bulk form, can be made ferroelectric when grown epitaxially on substrates such as cubic $KTaO_3$ (4.86% epitaxial compression). In such conditions, a $BaZrO_3$ thin film simulated at the DFT-LDA level presents a ferroelectric ground state of tetragonal (*P*4*mm*) symmetry with a band gap of 3.4 eV, *c*/*a* ratio of 1.12, spontaneous polarization of 53 μC/cm^2, and piezoelectric constant of 3.6 C/m^2, a set of values comparable to those experimentally reported for prototypical ferroelectrics such as $BaTiO_3$ or $PbTiO_3$. Starting from this, we built a Au/ZrO_2-(BaO-ZrO_2)$_m$/Au tunnel junction (Figure 1a) in which *m* layers of the ferroelectric material are sandwiched between symmetric gold electrodes.

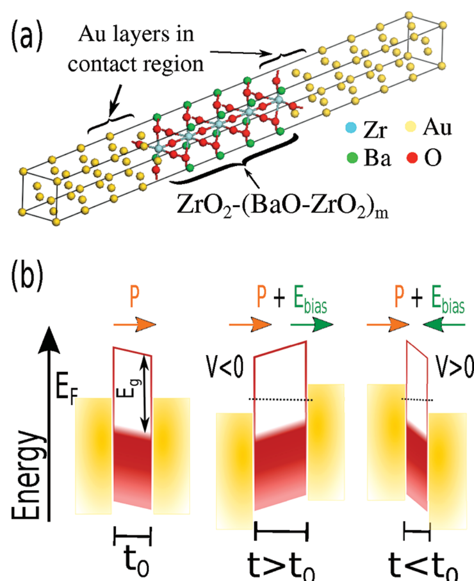

Figure 1. Sketch of our simulated s-FTJ. (a) Atomic view indicating the layers of the gold electrode that are explicitly considered in the contact region and are allowed to relax in response to the applied bias. (b) Energy profile along the tunneling barrier associated with a s-FTJ and its behavior under applied bias.

RESULTS AND DISCUSSION

The zero-bias equilibrium structure of our model s-FTJ was determined using the LDA as implemented in the code SIESTA.[27] The atomic positions and out-of-plane *c* lattice constant were optimized under fixed epitaxial strain conditions that mimic an in-plane compression of 4.86% (corresponding to the above-mentioned $KTaO_3$ (001) cubic substrate). Under short-circuit boundary conditions, the system remains ferroelectric for *m* values of 2 and 4, even though the screening of the depolarization field ($\mathcal{E}_{dep}$) is incomplete. As shown in Figure 2e (see the zero-bias result), this is reflected in a potential drop $\Delta V \simeq 110$ meV (30 meV) across the ferroelectric layer for $m = 4$ ($m = 2$), making the barrier trapezoidal. This situation is comparable to what was experimentally observed in strained $BaTiO_3$ films in ref 7. The reason why $\mathcal{E}_{dep}$ does not totally suppress the polarization of the barrier is two-fold: First, the epitaxially strained $BaZrO_3$ presents a relatively strong ferroelectric instability, with an associated energy double-well of about 106 meV per formula unit; second, gold electrodes on $BaZrO_3$ display good screening properties, with an effective

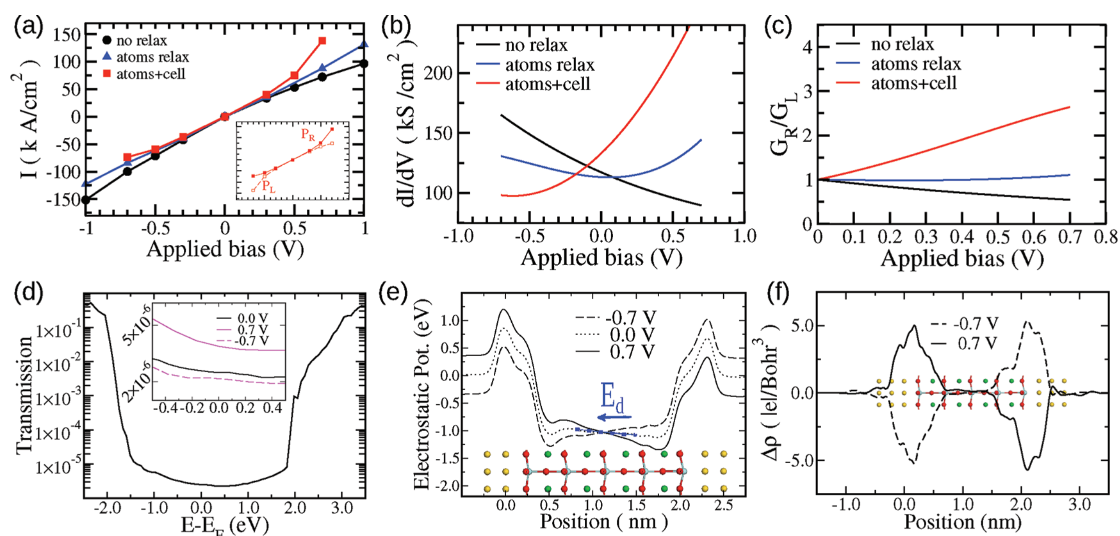

Figure 2. (a) $I-V$ curves corresponding to state R of our model s-FTJ (see text) and computed in various conditions: (1) Allowing a full ("atoms+cell") structural relaxation in response to applied bias (red); (2) allowing the atoms to relax but keeping the simulation cell fixed (blue); (3) fixing the zero-bias geometry (black). (b) Curves of dI/dV obtained by fitting the $I(V)$ data of panel (a). (c) Ratio of the differential conductances ($G = dI/dV$) of the R and L states of our s-FTJ (see text). (d) Transmission function at zero bias. The inset shows the region around $E - E_F = 0$, which determines the calculated intensities for the considered voltage values. The results for ± 0.7 V correspond to the atoms+cell case. (e) Position-dependent electrostatic potential for several voltage values (no relax case). (f) Position-dependent change of the electronic density $\Delta\rho$ with respect to zero-bias result (no relax case).

screening length of 0.037 Å. Finally, the Fermi level of the electrode is aligned with the middle of the gap of the ferroelectric, and the calculated Schottky barriers for electrons and holes ($\varphi_n = 1.80$ eV and $\varphi_p = -1.49$ eV, respectively) also agree well with what was reported in ref 28 and is expected for a typical metal/ferroelectric oxide interfaces.

We then performed a first-principles investigation of the transport properties of our s-FTJ. We used a non-equilibrium Green's function formalism combined with DFT[29] to calculate the electric current that appears in response to a *finite* bias potential. The methods, besides providing the current, also allow us to calculate the forces and stress induced by the external bias.[30] Our calculations, therefore, include for the first time both the electronic and lattice relaxations in response to the finite applied voltage. The computed $I-V$ and differential conductance ($G = dI/dV$) curves for $m = 4$ are shown in Figures 2a and 2b, respectively. We only show the case in which the polarization of the barrier is pointing to the right (state R), which is equivalent by symmetry with the case of a left-pointing polarization (state L). [The corresponding $I-V$ curves are related by $I^R(V) = -I^L(-V)$.] Also, as sketched in Figure 1b, we assume that a positive bias corresponds to having the left electrode at a higher potential. As a result, a positive bias produces an electric field pointing to the left and tends to depolarize the ferroelectric layer in state R.

The red curve of Figure 2a represents the expected $I-V$ characteristic of a FTJ in a finite bias, with a TER = I^R/I^L of 190% at $V = 0.7$ V. Further, the red dI/dV curves of Figure 2b provide an even stronger TER signature, as we obtain G_R/G_L ratios of about 2 already at a small bias of 0.5 V (see Figure 2c). This constitutes our main result and demonstrates that it is possible to achieve a sizable, experimentally detectable, TER effect in FTJs with symmetric electrodes.

These results correspond to the realistic situation in which the ferroelectric layer relaxes in response to the applied finite field (see sketch in Figure 1b). In fact, both the unit cell and the internal atomic positions are expected to relax significantly in ferroelectrics, which typically exhibit large piezoelectric and dielectric constants. In our case, the structural relaxation of the barrier as a function of applied voltage, obtained self-consistently in our first-principles calculations, can be reproduced accurately by a simple model, that is, an effective Hamiltonian that includes the ferroelectric soft-mode and strain degrees of freedom (see Supporting Information). For positive bias, the applied electric field goes against the polarization of the barrier, and consequently, the barrier thickness decreases *via* the inverse piezoelectric effect (-1.6% at $V = 0.7$ V). For negative bias, the opposite happens (a $+1.2\%$ barrier thickness increase at $V = -0.7$ V). Bearing this in mind, the general shape of the red $I-V$ curve in Figure 2a (*i.e.*, $I^R > I^L$) can be easily understood: under positive (negative) bias, the inverse piezoelectric effect results in a decrease (increase) of the thickness of the barrier, thus producing a concomitant increase (decrease) of the tunnel current, which depends exponentially on the barrier thickness.

To further demonstrate the role of the inverse piezoelectric effect, we performed additional calculations

under constrained geometries. More precisely, the black curves in Figures 2a–c were obtained by fixing the barrier and electrodes at the zero-bias geometry, and the blue curves correspond to an intermediate situation in which the atoms are allowed to relax while the total length of the simulated heterostructure along the *c* direction is kept fixed. This latter case mimics the experimental situation in which the FTJ is encapsulated, and although the thickness of the whole system is constrained, the atoms and the thickness of the ferroelectric layer can still slightly relax, thus compressing or expanding the electrodes.

Freezing the zero-bias geometry (black curves), the obtained $I-V$ characteristic is still notoriously asymmetric, with the current being larger for negative voltages. For example, at $V = 0.7$ V, we obtained a TER (I^R/I^L) of 70% and a G^R/G^L ratio of 0.5. Let us stress that this electroresistance effect has a purely electronic origin and directly emerges from the asymmetry of the barrier, imposed by the mere fact that it is polarized. Hence, this is a new and clear indication that having asymmetric electrodes may not be necessary to introduce a significant asymmetry in the current. Interestingly, note that the asymmetry associated with a purely electronic effect ($I^R < I^L$) is opposite to the one induced by the piezoelectric response ($I^R > I^L$). As a result of this competition, we obtain a rather symmetric result in the intermediate situation in which only a partial structural relaxation of the barrier was allowed (blue curves). The TER of the fully relaxed structure (red curves) results from the competition between electronic and inverse piezoelectric effects and is clearly dominated by the latter.

It is instructive to check whether our first-principles results can be captured by simple semiempirical models. In ref 16, a one-band model was used to estimate the $I-V$ curve of a rectangular piezoelectric barrier.[31] This model includes several physical parameters that were derived from experimental data by the authors of ref 16, but which we can alternatively obtain from first-principles. Using an average barrier height φ_0 = 1.85 eV, an effective piezoelectric constant d_{33} = −0.31 Å/V, a deformation potential of the conduction band κ_3 = 5.91 eV, and a barrier thickness at zero bias t_0 = 17.677 Å, all values directly derived from our calculations, we can fit the effective mass along the current flow (longitudinal direction, m_{30}) and its dependence on strain (μ_{33} coefficient) so that the model reproduces the first-principles $I-V$ curve in the fully relaxed case. We obtain a perfect agreement between this simple rectangular barrier model and the first-principles results (see Supporting Information) for m_{30} = 0.193m_e and μ_{33} = −0.827, where m_e is the free electron mass, which further supports our interpretation that the asymmetry of the current in our s-FTJ is dominantly produced by the piezoelectric response. Note that our fitted value of the effective mass is very close to the value used in ref 16 (m_{30} = 0.2m_e). It is, however, significantly smaller than the band mass we can extract from the dispersion curves of $BaZrO_3$ (m_l = 2.86m_e and m_t = 0.38m_e for the lowest conduction band). This artificially low value can be understood as a renormalization of the mass required to compensate for at least two effects: First, there are both electron and hole contributions to the current, which translate within this simple one-band picture in a decrease of the effective mass. In fact, the transmission function computed from first-principles suggests that the hole contribution is slightly dominant (see Figure 2d for representative results). Second, $BaZrO_3$ is not insulating in the interfacial region, and the effective thickness of the barrier is probably smaller than the physical thickness included in the model; a smaller mass can also effectively compensate for the overestimate of the barrier thickness.

In ref 32, an alternative model was used that includes an intrinsic asymmetry of the FTJ through the consideration of a trapezoidal barrier. In principle, in our s-FTJ, the asymmetry of the barrier should be coming from the incomplete screening of the depolarizing field, which yields a difference of barrier height between the left and right interfaces of ΔV = 110 meV for $m = 4$. If we combine the two models to properly include both this intrinsic asymmetry and the piezoelectric effect, we get again a proper description of the first-principles $I-V$ curves (see Supporting Information) with parameters relatively similar to those obtained for the rectangular barrier (m_{30} = 0.197m_e and μ_{33} = −1.292). This reflects the fact that the intrinsic asymmetry of the barrier is small and has a minor impact on the shape of the current. Accordingly, if we now set the piezoelectric coefficient to zero, we do not get any sizable asymmetry (TER $\approx$ 100%) in the $I-V$ curve, which implies that a simple trapezoidal barrier cannot fit the asymmetry obtained at fixed zero-bias geometry. This suggests that the intrinsic asymmetry is a rather complex effect, going beyond the simple presence of a depolarizing field and probably more related to interfacial effects.

It is interesting to try to get better insight into this purely electronic TER effect, for which our first-principles simulations suggest the following qualitative explanation. As shown in Figures 2e and 2f, the right interface seems electronically more reactive to an applied bias, especially with regard to the penetration into the ferroelectric barrier of the bias-induced $\Delta\rho$. Such a differentiated behavior of the left and right interfaces relies on their different atomic structures, which is, in turn, a consequence of the presence of a spontaneous polarization; for example, because the polarization of our simulated s-FTJ points from left to right (see Figure 1b), the right interface presents relatively short Zr–Au bonds (3.13 Å) as compared with the left one (3.30 Å). Then, in our simulations,

application of a negative (positive) bias results in an increased electronic density at the right (left) interface, which leads to a relatively large (small) charge *leakage* into the barrier, and thus a large (small) current. We can thus rationalize the sign of the purely electronic TER effect shown in Figure 2 in terms of a mechanism that might apply to other FTJs, as well. Further work will be needed to confirm such a mechanism and its generality.

Finally, let us comment on how the TER effect we have obtained compares with values in the literature. The very large TER values of 75 000% reported by García *et al.*[7] for strongly asymmetric FTJs were measured at very large biases (1.5−2.5 V) that probably lie beyond the switching voltage of our s-FTJ (see Supporting Information). Thus, we doubt such large effects can be reached in a s-FTJ as ours, even if thicker junctions were considered. On the other hand, in their seminal paper,[14] Zhuravlev *et al.* estimated a $G_R/G_L \approx 4$ at 0 V for a typical a-FTJ that was 1 nm thick and had a spontaneous polarization of 50 μC/cm^2. In contrast, our s-FTJ renders a $G_R/G_L \approx 2$ at a bias of 0.5 V. This suggests that s-FTJs may be an alternative to a-FTJs for low-power applications, as they exhibit competitive TER values at small applied bias.

CONCLUSIONS

In summary, our first-principles study gives compelling evidence that it is possible to achieve a relatively large tunneling electroresistance in ferroelectric tunnel junctions with symmetric electrodes. We have shown that the asymmetry of the current is essentially controlled by the piezoelectric response of the junction to an applied bias. Our simulations also reveal an intrinsic asymmetry that seems related to complex interfacial effects. In our model system, the two types of asymmetry compete. Better understanding the origin of the intrinsic asymmetry would be valuable and might help to identify systems in which intrinsic and piezoelectric mechanisms cooperate in order to yield even larger TER values.

METHODS

The zero-bias calculations have been performed within DFT and using LDA as implemented in SIESTA code.[27] The electronic transport calculations in finite applied bias were performed using the non-equilibrium Green's function formalism combined with DFT[29] as implemented in TranSIESTA code. We use a simple Hamiltonian model, which includes the ferroelectric soft-mode and strain degrees of freedom, in order to describe the atomic and strain relaxations of the symmetric FTJs. The semiempirical one-band models for a rectangular piezoelectric and trapezoidal ferroelectric barriers were used to fit the first-principles tunneling currents (see Supporting Information for technical details and references).

Acknowledgment. This work was supported by the EC-FP7 project OxIDes (Grant No. CP-FP 228989-2). Work at ULG was also funded by the IAP Program of the Belgian State-Belgian Science Policy (Grant No. P6/42). Work at the ICMAB was also funded by MICINN-Spain (Grant Nos. MAT2010-18113, MAT2010-10093-E, and CSD2007-00041). Work at the CIN2 was also funded by MICINN-Spain (Grant Nos. FIS2009-12721-C04 and CSD2007-00050). F.D.N. was partly supported by the *Juan de la Cierva* program of MICINN-Spain. P.G. acknowledges professorship from the Francqui Foundation.

Supporting Information Available: More technical details and additional informations are reported separately. This material is available free of charge *via* the Internet at http://pubs.acs.org.

REFERENCES AND NOTES

1. Chang, L. L.; Esaki, L. Nonvolatile Schottky Diode with Barrier Height Controlled by Ferroelectric Polarization. *IBM Tech. Discl. Bull.* **1971**, *14*, 1250.
2. Junquera, J.; Ghosez, Ph. First-Principles Study of Ferroelectric Oxide Epitaxial Thin Films and Superlattices: Role of the Mechanical and Electrical Boundary Conditions. *J. Comput. Theor. Nanosci.* **2008**, *5*, 2071–2088.
3. Stengel, M.; Vanderbilt, D.; Spaldin, N. A. Enhancement of Ferroelectricity at Metal-Oxide Interfaces. *Nat. Mater.* **2009**, *8*, 392–397.
4. Contreras, J. R.; Kohlstedt, H.; Poppe, U.; Waser, R.; Buchal, C.; Pertsev, N. A. Resistive Switching in Metal-Ferroelectric-Metal Junctions. *Appl. Phys. Lett.* **2003**, *83*, 4595–4597.
5. Gajek, M.; Bibes, M.; Fusil, S.; Bouzehouane, K.; Fontcuberta, J.; Barthélémy, A.; Fert, A. Tunnel Junctions with Multiferroic Barriers. *Nat. Mater.* **2007**, *6*, 296–302.
6. Scott, J. F. Ferroelectric Memories. *Springer Series in Advanced Microelectronics*; Springer-Verlag: Berlin, 2000; Vol. 3.
7. García, V.; Fusil, S.; Bouzehouane, K.; Enouz-Vedrenne, S.; Mathur, N. D.; Barthélémy, A.; Bibes, M. Giant Tunnel Electroresistance for Non-destructive Readout of Ferroelectric States. *Nature* **2009**, *460*, 81–84.
8. Gruverman, A.; Wu, D.; Lu, H.; Wang, Y.; Jang, H. W.; Folkman, C. M.; Zhuravlev, M. Ye.; Felker, D.; Rzchowski, M.; Eom, C.-B.; *et al.* Tunneling Electroresistance Effect in Ferroelectric Tunnel Junctions at the Nanoscale. *Nano Lett.* **2009**, *9*, 3539.
9. Zheng, Y.; Woo, C. H. Giant Piezoelectric Resistance in Ferroelectric Tunnel Junctions. *Nanotechnology* **2009**, *20*, 075401.
10. Maksymovych, P.; Jesse, S.; Yu, P.; Ramesh, R.; Baddorf, A. P.; Kalinin, S. V. Polarization Control of Electron Tunneling into Ferroelectric Surfaces. *Science* **2009**, *324*, 1421–1425.
11. Hambe, M.; Petraru, A.; Pertsev, N. A.; Munroe, P.; Nagarajan, V.; Kohlstedt, H. Crossing an Interface: Ferroelectric Control of Tunnel Currents in Magnetic Complex Oxide Heterostructures. *Adv. Funct. Mater.* **2010**, *20*, 2436–2441.
12. Crassous, A.; García, V.; Bouzehouane, K.; Fusil, S.; Vlooswijk, A. H. G.; Rispens, G.; Noheda, B.; Bibes, M.; Barthélémy, A. Giant Tunnel Electroresistance with $PbTiO_3$ Ferroelectric Tunnel Barriers. *Appl. Phys. Lett.* **2010**, *96*, 42901.
13. García, V.; Bibes, M.; Bocher, L.; Valencia, S.; Kronast, F.; Crassous, A.; Moya, X.; Enouz-Vedrenne, S.; Gloter, A.; Imhoff, D.; *et al.* Ferroelectric Control of Spin Polarization. *Science* **2010**, *327*, 1106–1110.
14. Zhuravlev, M. Y.; Sabirianov, R. F.; Jaswal, S. S.; Tsymbal, E. Y. Giant Electroresistance in Ferroelectric Tunnel Junctions. *Phys. Rev. Lett.* **2005**, *94*, 246802.
15. It may be difficult to switch an a-FTJ transform into its unfavoured high-energy polarization state, which will be a source of imprint.
16. Kohlstedt, H.; Pertsev, N. A.; Contreras, J. R.; Waser, R. Theoretical Current−Voltage Characteristics of Ferroelectric Tunnel Junctions. *Phys. Rev. B* **2005**, *72*, 125341.
17. Zimbovskaya, N. A. Electron Transport through Asymmetric Ferroelectric Tunnel Junctions: Current−Voltage Characteristics. *J. Appl. Phys.* **2009**, *106*, 124101.

18. Wu, Y. Z.; Ju, S.; Li, Z. Y. Effects of Electrodes and Space Charges on the Tunneling Electroresistance in the Ferroelectric Tunnel Junction with a $SrTiO_3$/$BaTiO_3$ Composite. *Appl. Phys. Lett.* **2010**, *96*, 252905.
19. Tsymbal, E. Y.; Kohlstedt, H. Tunneling Across a Ferroelectric. *Science* **2006**, *313*, 181–183.
20. Velev, J. P.; Duan, C. G.; Belashchenko, K. D.; Jaswal, S. S.; Tsymbal, E. Y. Effect of Ferroelectricity on Electron Transport in Pt/$BaTiO_3$/Pt Tunnel Junctions. *Phys. Rev. Lett.* **2007**, *98*, 137201.
21. Luo, X.; Lin, S. P.; Wang, B. A.; Zheng, Y. Impact of Applied Strain on the Electron Transport through Ferroelectric Tunnel Junctions. *Appl. Phys. Lett.* **2010**, *97*, 012905.
22. Burton, J. D.; Tsymbal, E. Y. Giant Tunneling Electroresistance Effect Driven by an Electrically Controlled Spin Valve at a Complex Oxide Interface. *Phys. Rev. Lett.* **2011**, *106*, 157203.
23. Caffrey, N. M.; Archer, T.; Rungger, I.; Sanvito, S. Prediction of Large Bias-Dependent Magnetoresistance in All-Oxide Magnetic Tunnel Junctions with a Ferroelectric Barrier. *Phys. Rev. B* **2011**, *83*, 125409.
24. Luo, X.; Wang, B.; Zheng, Y. Tunable Tunneling Electroresistance in Ferroelectric Tunnel Junctions by Mechanical Loads. *ACS Nano* **2011**, *15*, 1649–1656.
25. Symmetric junctions were considered by Velev *et al.*,[20] who discussed various interface effects; yet, these authors did not compute the TER, as for s-FTJs this requires simulations at finite bias.
26. Stengel, M.; Aguendo-Puente, P.; Spaldin, N. A.; Junquera, J. Band Alignment at Metal/Ferroelectric Interfaces: Insights and Artifacts from First Principles. *Phys. Rev. B* **2011**, *83*, 235112.
27. Soler, J. M.; Artacho, E.; Gale, J. D.; Garcia, A.; Junquera, J.; Ordejón, P.; Sanchez-Portal, D. The SIESTA Method for *Ab Initio* Order-N Materials Simulation. *J. Phys.: Condens. Matter* **2002**, *14*, 2745–2779 (http//www.icmab.es/siesta).
28. Hartmann, A. J.; Neilson, M.; Lamb, R. N.; Watanabe, K.; Scott, J. F. Ruthenium Oxide and Strontium Ruthenate Electrodes for Ferroelectric Thin-Film Capacitors. *Appl. Phys. A* **2000**, *70*, 239–242.
29. Brandbyge, M.; Mozos, J. L.; Ordejón, P.; Taylor, J.; Stokbro, K. Density-Functional Method for Nonequilibrium Electron Transport. *Phys. Rev. B* **2002**, *65*, 165401.
30. Brandbyge, M.; Stokbro, K.; Taylor, J.; Mozos, J. L.; Ordejón, P. Origin of Current-Induced Forces in an Atomic Gold Wire: A First-Principles Study. *Phys. Rev. B* **2003**, *67*, 193104.
31. Brinkman, W. F.; Dynes, R. C.; Rowell, J. M. Tunneling Conductance of Asymmetrical Barriers. *J. Appl. Phys.* **1970**, *41*, 1915.
32. Simmons, J. G. Electric Tunnel Effect between Dissimilar Electrodes Separated by a Thin Insulating Film. *J. Appl. Phys.* **1963**, *34*, 2581.